



Research papers

Interaction effects of rainfall and soil factors on runoff, erosion, and their predictions in different geographic regions



Qihua Ke, Keli Zhang*

State Key Laboratory of Earth Surface Processes and Resource Ecology, School of Geography, Faculty of Geographical Science, Beijing Normal University, Xinjiekouwai St. 19, 100875 Beijing, China

ARTICLE INFO

This manuscript was handled by Jiri Simunek, Editor-in-Chief, with the assistance of Jian Luo, Associate Editor.

Keywords:

Factor interaction
Prediction uncertainty
Soil erodibility
Runoff-ability
Mesoplot scale
Structural equation modeling

ABSTRACT

Water erosion is a complex process driven by many factors, such as rainfall, soil, topography, vegetation, and land use management practices. Much research has been done to assess the separate effect of every single factor, while studies devoted to the interaction effects among these factors are rarely reported. The complex interactions among factors are generally poured into the pool of soil erodibility (K factor) in the USLE-based models, which induces uncertainty of the K factor and thus causes prediction errors. The interaction between rainfall (R) and soil (K) factors is the first and foremost step to dissect the entire interaction complex, but also the objective this study intended to investigate. Quality-controlled data from long-term field observations on four bare steep slopes in different geographic regions of China were selected and standardized to exclude the effect of unconcerned factors. The interaction effects of rainfall and soil factors were visualized by the nonlinearities of accumulative rainfall-runoff-erosion relationships and then further quantified by the evaluation of prediction errors for the cases that ignore the nonlinearities and by the approach of partial least squares-structural equation modelling (PLS-SEM). The results indicated that the interaction between rainfall and soil factors exists in water erosion processes and obscures the hydrological and erosion prediction. (1) The potentialities of both runoff and erosion varied with the level of rainfall erosivity in different patterns among soils, indicating diverse nonlinearities of rainfall-runoff-erosion relationships and the complex interaction effects behind it. (2) The addition of the interaction effects in the SEM model constructions increased 9.2% and 6.0% of variance explanations for the predictions of annual runoff and erosion, respectively. Whereas, the exclusion of interaction effects tended to cause overestimations on steep slopes that were hard to be calibrated by existing formulas. (3) The well-known tendency to underestimate small and overestimate large events does not suit every soil, especially for the soil with coarse texture and shallow soil with fractured bedrock. And prediction bias was found predictable and rooted in the interaction between rainfall and soil. This study yields a deeper understanding of interaction effects, and is helpful for the improvement of runoff and erosion predictions.

1. Introduction

Soil erosion is a global environmental issue that triggers the loss of fertile topsoil and threatens food safety in many parts of the world (Pimentel, 2006). How to assess or predict soil loss reliably and precisely has always been very a Gordian knot ever since the beginning of soil erosion research (Trimble and Crosson, 2000; Parsons, 2019). Even the most successful water erosion model, the Universal Soil Loss Equation (USLE) (Wischmeier and Smith, 1978), has been widely reported that there were considerable errors when it was applied to estimate soil loss in different regions, countries, and continents (Zhang et al., 2016;

Benavidez et al., 2018; Alewell et al., 2019). The complex interactions among erosion factors have been considered as a significant source of the prediction uncertainty (Wischmeier, 1976; Beven and Brazier, 2011; Benavidez et al., 2018). Soil erosion by rainfall and runoff is a complex process affected by many factors. The USLE estimates water erosion by multiplying the values of the six factors.

$$A = R \times K \times L \times S \times C \times P \quad (1)$$

Where A is the average annual soil loss ($t \cdot hm^{-2} \cdot yr^{-1}$), R is the rainfall and runoff factor, also termed as rainfall erosivity index ($MJ \cdot mm \cdot hm^{-2} \cdot h^{-1}$), K is the soil erodibility factor ($t \cdot h \cdot MJ^{-1} \cdot mm^{-1}$), L is

* Corresponding author.

E-mail addresses: qihuake@mail.bnu.edu.cn (Q. Ke), keli@bnu.edu.cn (K. Zhang).

the slope length factor (unitless), S is the slope gradient factor (unitless), C is the cover-management factor (unitless), P is the conservation practice (unitless). In which the R is the base value that denotes the potential erosive energy of rainfall and runoff induced by rainfall; K is the base value that represents the intrinsic susceptibility of a specific soil to erosion by raindrop splash and runoff wash during rainfall; the other four factors (L , S , C , P) are multipliers that outline the environment, namely the media that accommodates erosion processes.

Previous studies have primarily been focused on the separate effect of every single factor; however, very few research has been devoted to the effects of multi-factor interactions on water erosion (Hua et al., 2019). This contrast reflects the fact that most erosion models have a major intrinsic limitation that they basically neglect the complex interactions among factors in order to distinguish more easily the individual effect of each factor (Roose, 1996). However, in the context of bottlenecked prediction accuracy, there is a growing consensus that soil erosion is a complex process determined by the mutual interaction of many factors (Cebecauer and Hofierka, 2008). Also, there is a growing need now to disentangle the complex interactions among factors (Estrada-Carmona et al., 2017) and factor the interaction effects into the model construction (Hua et al., 2019; Raza et al., 2021). Thus it's necessary to assess the prediction uncertainty that results from the interactions among the six factors in the application of USLE-based models.

The first and basic step into the dissection of the interaction complex is to explore the interaction between the rainfall factor (R) and soil factor (K) on the standard plot. The USLE defines soil erodibility (K) as the rate of soil loss per unit of rainfall erosion index for a specific soil as measured on a unit plot, which is a plot that is a 22.13 m length ($L = 1$) of uniform 9% slope ($S = 1$) in continuous fallow condition ($C = 1$) with up-and-down clean tillage ($P = 1$) and no new input of organic matter for at least three years (Roose, 1996). Thus the K value for a specific soil is measured as the following equation:

$$K = \frac{A}{R} \quad L = S = C = P = 1 \quad (2)$$

In which A is the average annual soil loss measured from plot sediment data, R is the average annual rainfall erosivity index calculated from the rainfall records; while K is the only value that is unknown and uncertain. This definition implies that the soil erodibility K is a black-box coefficient that integrates the complex interactions among the six factors and takes over all the corresponding uncertainties. This model design that pours all the interaction effects into the pool of soil erodibility K factor induces uncertainty of the K factor and thus causes inherent prediction errors for USLE-based models. This is why some researchers attributed the prediction errors to the uncertainties in soil erodibility (Borselli et al., 2012). According to the definition of soil erodibility, the value of K is embodied in the long-term interactions that rainfall acts on the soil and reversely soil reacts to rainfall. Thus the interaction between rainfall (R) and soil (K) is the fundamental structure of the complex interactions that exist among erosion factors.

However, few studies have been conducted to focus on the interaction between rainfall and soil, and even rare in terms of a quantitative assessment of the interaction effect. Most attention has been paid to assess rainfall factor and soil factor separately (Fox and Bryan, 1992; Nishigaki et al., 2017). Several studies that concern the interaction typically only emphasize that soil crust is a result of the interactions and it affects hydrological and erosion processes through altering surface conditions (Chamizo et al., 2012; Issa et al., 2011; Le Bissonnais et al., 1995). Thus a deeper insight into the mechanism of the interaction between rainfall and soil and quantitative assessment of the interaction effect is very urgent.

The complex interactions between the soil and rainfall determine the processes and yields of runoff and erosion (Borselli et al., 2012). This study hypothesizes that the interaction effects of rainfall and soil factors exist in the hydrological and erosion processes and thus lead to

substantial uncertainty in the predictions of runoff and erosion. Thus, the main objectives of this research were to identify the existence of interaction between rainfall and soil and to quantify the prediction uncertainties induced by the interaction effects. To achieve the goal, the specific objectives are as follows: (1) to examine how the interaction between rainfall and soil affects the hydrological and erosion processes; (2) to assess how many prediction biases were induced by the interaction effect; (3) to identify whether the interaction effect reached a statistically significant level or not. This work may be helpful for a better understanding of the mechanism of the rainfall-soil interaction and the pathway the interaction causes prediction uncertainties.

2. Materials and methods

2.1. Plot sites selection

Four typical stations were selected in the four regions with different geographical conditions, namely the northwestern loess plateau region, southwestern purple soil region, southwestern karst region, and southern red soil region (Fig. 1). These four regions represent the main water erosion area under the hilly context in China and meanwhile differ in climate, terrain, lithology, soil, and vegetation (Wang et al., 2015). To increase the possibility of detection of the interaction effects, a steep slope that has a higher magnitude of yield and variation in soil loss (El Kateb et al., 2013) is a better choice than a gentle one. Thus bare field plots with similar steep slopes were selected for each station. Detailed information of basic climate index, soil properties, and observation specifications for the four bare steep plots is listed in Table 1.

2.2. Data collection

We obtained 3–5 years of observations on the rainfall, runoff, and sediment during 1985–2014 for each plot. Rainfall data were automatically and continuously recorded by a rain gauge near the runoff plot. Runoff and sediment samples were artificially collected from the runoff plot after each rainfall event. All the four plots were arranged with the demands for the management of unit plot. Records from the first two years after the plot construction and the rainfall events with no runoff or sediment were excluded to avoid distortions. All the records were checked and corrected if there were any omissions or mistakes. Finally, a total of 17 plot-years of 227 event records from natural rainstorms were collected (Table 1). And the soil depth and lithology data were measured on the plot during the construction period.

The input data for the partial least squares-structural equation modeling (PLS-SEM) are composed of unvarying values of soil indexes, and annual values of rainfall, runoff, and sediment data. The soil data at each site was compiled from the existing plot information, scientific journal articles (Jiang et al., 2020; Ruan et al., 1995; Sheng et al., 2016; Zhao et al., 2013), academic dissertations (Gu, 2004; He, 2007), and Harmonized World Soil Database (HWSD V1.2) (FAO et al., 2012). The rainfall, runoff, and sediment data were prepared with annual values based on the collected 17 plot-years records from the four stations plus another 8 plot-years records at Yuexi (a station similar to Anxi) from the early work (Ke and Zhang, 2021). In total, 5 samples for soil data and 25 samples for annual rainfall, runoff, and sediment data were obtained. More details of PLS-SEM will be explained in section 2.4.2.

As for the map data (Fig. 1), 30 years (1986–2015) of daily precipitation records were used to delineate the spatial distribution of annual rainfall erosivity in China. Besides, the soil and water conservation regionalization map of China was obtained from the raw data in a published paper (Wang et al., 2018).

2.3. Data standardization

To compare the interaction patterns in different geographic regions, the effects from differences in topography and rainfall regimes should be



Fig. 1. Geographical location of stations. Regionalization of soil and water conservation in China in this map refers to the national plan of soil and water conservation of China released in 2012.

Table 1
Information for runoff plots.

Plot	Geographic region	Climate		Soil conditions									Plot observations			
		P (mm)	T (°C)	Soil name	Soil type	Sand (%)	Silt (%)	Clay (%)	SOM (%)	WSAC (%)	Gravel (%)	Depth (cm)	L (m)	S (°)	Plot years	Storm cases
Ansai	Northwestern Loess Plateau region	505	8.8	Loess soil	Ustorthents	14.5	70.6	14.9	0.18	23.4	8	>200	20	15	5	39
Suining	Southwestern purple soil region	993	17.4	Purple soil	Eutrudepts	25.8	52.4	21.8	1.28	80.7	16	40	20	15	5	35
Bijie	Southwestern karst region	863	14	Karst soil	Paleudults	26.1	32.9	41.0	3.44	93.6	24	21	20	15	3	60
Anxi	Southern red soil region	1600	20	Red soil	Kandiudults	49.0	24.8	26.2	0.78	37.1	3	>100	16.7	14	4	93

Note: Soil type is at the great group level in the USDA soil taxonomy (ST) classification system. The lithology of the bedrock underlying the thin Purple soil and Karst soil is sand-shale and limestone, respectively. Size ranges of sand, silt, and clay refer to the USDA soil particle-size classification system. P: annual precipitation; T: annual temperature; SOM: soil organic matter; WSAC: water-stable aggregate content (>0.25 mm); L: slope length; S: slope gradient.

eliminated by data standardization.

2.3.1. Standardization of the topographic factor

In the cases that the runoff plot data need to be calibrated to the unit plot with 22.13 m length and 9% slope gradient, the equations refer to Chinese Soil Loss Equation (CSLE) algorithms (Liu et al., 1994; Liu et al., 2000; Liu et al., 2002). For the cross-geographic-region comparisons in runoff and erosion, the topographic factors were normalized to 20 m length and 15° (26.2%) slope gradient by referring to the standard of unit plot in China (Zhang et al., 2000) with the transformed equations in our previous work (Ke and Zhang, 2021).

2.3.2. Standardization of the rainfall factor

To remove the influences of diversities in the frequency distribution of raindrop size, rainfall intensity and rainfall amount, the standardization of the rainfall factor is also necessary. Rainfall erosivity (R), namely EI_{30} , is the most frequently used index for the potentiality of a rainstorm to cause erosion due to its excellency in explaining the variation in soil loss (Wischmeier, 1959). However, the optimum indicator for the potentiality of a rainfall event to induce runoff still reaches no consensus. To determine an appropriate indicator, correlation and regression analyses of plot data in 227 rainstorms were performed. The results suggested that rainfall erosivity EI_{30} is the most closely correlated rainfall index for both runoff and erosion with Spearman correlation coefficients of 0.82 and 0.79, respectively ($p < 0.01$). Moreover, rainfall erosivity EI_{30} could explain 78.0% and 72.0% of the variabilities in runoff and erosion, respectively ($p < 0.01$). Thus index EI_{30} can not only embody the effect of rainfall on erosion but also runoff. Therefore, the rainfall erosivity EI_{30} was selected as the rainfall factor to represent the effect of rainfall on surface runoff and soil loss. The calculation of EI_{30} refers to the algorithm of Brown and Foster (1987) in the RUSLE model.

2.4. Methods for interaction detection

2.4.1. Factorial design

Factorial designs allow the analysis of the main effect (also called a simple effect) of each factor, as well as the effect of interactions between factors on the target. Rainfall erosivity and soil type were set as the rainfall factor and soil factor in the factorial design. The main effects of rainfall and soil were directly testified by the linearity of rainfall-runoff-erosion relationships. Furthermore, the interaction effects of rainfall and soil were visualized by the non-linearities (breaks) in double-mass curves of rainfall-runoff-erosion with cumulative data in the order of rainfall size. A continuous least-square piecewise linear regression approach was used to identify the critical point (break in the slope) and then divide the double-mass curve into two or three linear segments. The ratio b_n/b_{n-1} was used to reflect the degree of the change between the slope of the segment before the break (b_{n-1}) and the slope of the segment after the break (b_n). This study used a 20% difference in the slope as the criterion of significant change, thus b_n/b_{n-1} smaller than 0.80 or larger than 1.20 indicated a significant change.

Table 2

Segmental errors in surface runoff estimation for individual rainstorms using the $r = R^*ra$ method.

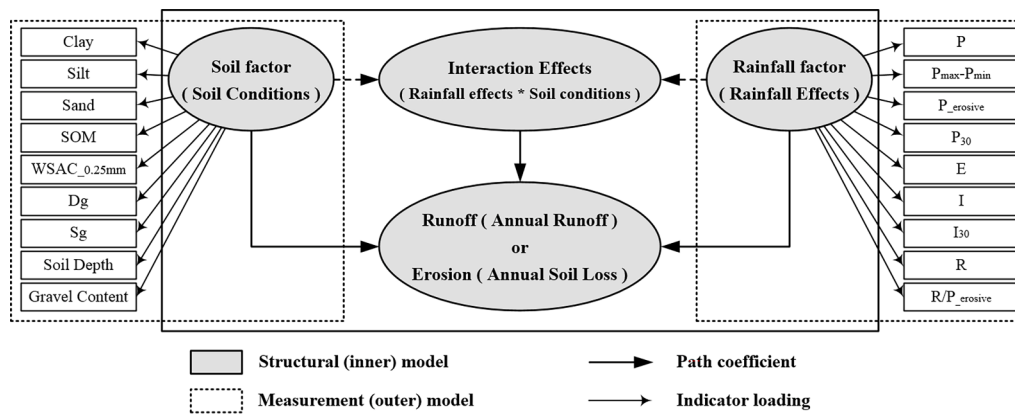
Soil description	Runoff-ability ra (mm·h·hm ⁻² ·MJ ⁻¹ ·mm ⁻¹)	Rainfall erosivity range (MJ·mm·hm ⁻² ·h ⁻¹)	Over-predicted events (%)	Under-predicted events (%)	OPE (%)	MAE (mm)
Loess soil	0.0064	$R \leq 640.8$	43.2	56.8	-14.3	1.4
		$R > 640.8$	100.0	0.0	17.3	10.3
Purple soil	0.0125	$R \leq 506.5$	74.2	25.8	53.3	5.3
		$R > 506.5$	0.0	100.0	-36.2	26.8
Karst soil	0.0063	$R \leq 180.8$	29.8	70.2	-55.9	1.6
		$R > 180.8$	70.0	30.0	28.5	9.9
Red soil	0.0124	$R \leq 330.2$	8.6	91.4	-42.3	4.9
		$R > 330.2$	60.9	39.1	21.8	24.6

Note: Runoff-ability, ra , is the runoff depth induced by unit rainfall erosivity on the unit plot that is 22.13 m length of uniform 9% slope in continuous fallow condition with up and downslope clean tillage. r : runoff depth; R : rainfall erosivity. OPE: overall percentage errors; MAE: mean absolute error.

Table 3Segmental errors in soil loss estimation for individual rainstorms using the $A = R^*K$ method.

Soil description	Soil erodibility K (t·hm ² ·h·hm ⁻² ·MJ ⁻¹ ·mm ⁻¹)	Rainfall erosivity range (MJ·mm·hm ⁻² ·h ⁻¹)	Over-predicted events (%)	Under-predicted events (%)	OPE (%)	MAE (t·hm ⁻²)
Loess soil	0.0095	$R \leq 640.8$	73.0	27.0	22.2	2.5
		$R > 640.8$	0.0	100.0	-13.9	16.6
Purple soil	0.0030	$R \leq 506.5$	77.4	22.6	53.5	1.7
		$R > 506.5$	0.0	100.0	-36.2	6.5
Karst soil	0.0029	$R \leq 180.8$	95.7	4.3	176.6	0.3
		$180.8 < R \leq 1090.8$	25.0	75.0	-33.0	4.1
		$R > 1090.8$	100.0	0.0	15.3	5.0
Red soil	0.0084	$R \leq 660.5$	14.1	85.9	-40.7	4.5
		$R > 660.5$	86.7	13.3	39.0	25.3

Note: Soil erodibility factor K , soil loss caused by unit rainfall erosivity on the unit plot that is 22.13 m length of uniform 9% slope in continuous fallow condition with up and downslope clean tillage. A : soil loss; R : rainfall erosivity. OPE: overall percentage errors; MAE: mean absolute error.



fall energy; I : mean annual rainfall intensity; I_{30} : mean annual maximum 30-minute intensity; R : annual rainfall erosivity; R/P_{erosive} : annual rainfall erosivity caused by one unit annual erosive rainfall amount.

2.4.2.1. PLS-SEM model construction. The PLS-SEM consists of two sub-models: the structural model and measurement model (Fig. 2). The inner model, namely the structural model, interprets the relationships between constructs and endogenous latent variables. We constructed a two-factor interaction model with three constructs (*Rainfall Effects*, *Soil Conditions*, and their cross-product *Interaction Effects*) and two endogenous latent variables (*Annual Runoff* and *Annual Soil Loss*). Here we hypothesized that the *Interaction Effects* (i.e., *Rainfall Effects***Soil Conditions*) exert significant impacts on the *Annual Runoff* and *Annual Soil Loss*. The outer model, namely measurement model, describes the relationships between the latent and observed variables. We selected nine reflective indicators as the observed variables for the latent variables *Rainfall Effects* and *Soil Conditions*, respectively. The *Soil Conditions* were measured by soil texture (Clay, Silt, Sand, Dg, Sg), soil water retention and aggregation stability (SOM, WSAC_{0.25mm}), soil mass (Soil depth), and rock fragment (Gravel content). The *Rainfall Effects* were reflected by precipitation amount (P , $P_{\max}-P_{\min}$), erosive rainfall amount (P_{erosive} , P_{30}), rainfall energy (E), rainfall intensity (I , I_{30}), rainfall erosivity (R , R/P_{erosive}). We implemented the PLS-SEM analyses with the moderating effect module in SmartPLS 3.0 (<https://www.smartpls.com/>) to test the above hypothesized relationships.

2.4.2.2. PLS-SEM model evaluation.

(1) Measurement model evaluation

The measurement model evaluation is to examine the quality of indicators. Here we focus on the reliability of the indicators for the rainfall and soil factors. The indicator loading denotes correlations between

Fig. 2. Conceptual partial least squares structural equation modeling (PLS-SEM) model specification. The interaction effect means the pairwise product term between the 9 indicators of Soil Conditions and the 9 indicators of Rainfall Effects. SOM: soil organic matter; WSAC_{0.25mm}: water-stable aggregate content (>0.25 mm); Dg: geometric mean particle diameter; Sg: the logarithm of geometric standard deviation of geometric size of the particle size; P : annual precipitation; $P_{\max}-P_{\min}$: the difference in maximum and minimum monthly precipitation; P_{erosive} : annual total precipitation of storms causing soil loss; P_{30} : annual total precipitation from the part of maximum 30-minute intensity above 30 mm/h; E : annual rainfall energy; I : mean annual rainfall intensity; I_{30} : mean annual maximum 30-minute intensity; R : annual rainfall erosivity; R/P_{erosive} : annual rainfall erosivity caused by one unit annual erosive rainfall amount.

each latent variable and the observed variable. The individual indicator reliability that is calculated by squaring the indicator loading denotes an indicator's variance that can be explained by the underlying latent variable, for which a value over 0.4 is regarded as satisfactory in a reflective model (Hulland, 1999).

(2) Structural model evaluation

Path coefficient (β), coefficient of determination (R^2), and Stone-Geisser's Q^2 values can assess the explanatory power of the structural model. The β represents the influence of constructs on endogenous latent variables (equivalent to standardized regression coefficients), which can examine the direction and strength of causal linkages (Grace, 2006). The R^2 represents the goodness of fit for the model, which ranges from 0 to 1, and the values of 0.10, 0.25, 0.50, 0.75 can be regarded as insignificant, weak, moderate, and substantial, respectively (Hair Jr et al., 2016). Q^2 value from the blindfolding procedure is a criterion of the model's predictive capability. The higher the Q^2 value and the higher the model's predictive capability (Chin, 2010).

(3) Effect size evaluation

The effect size (f^2) is a useful way to detect whether a construct has a substantive impact on the endogenous variable. In the testing for interaction effects using PLS-SEM, we followed a hierarchical process that compares the R^2 results of two models, namely the main effect model (the model without interaction) and the interaction model (Limayem et al., 2001). The effect size of the interaction effects was suggested to be assessed by the Cohen effect size formula (Cohen, 1998).

$$f^2 = \frac{R^2_{\text{with interaction}} - R^2_{\text{without interaction}}}{1 - R^2_{\text{with interaction}}} \quad (7)$$

Where f^2 is the effect size of interaction; $R^2_{\text{with interaction}}$ is the R^2 of the interaction model; $R^2_{\text{without interaction}}$ is the R^2 of the model without the interaction term. Interaction effects with f^2 of 0.02, 0.15, and 0.35 have been suggested as small, medium, and large effects respectively (Cohen, 1998). Besides the interaction effects, the effect size f^2 of the simple main effects of Rainfall Effects and Soil Conditions were also used to assess whether they have substantive influences on the annual yield of runoff and erosion. The calculation refers to the algorithm of BoBöw-Thies and Albers (2010).

(4) Significance test

The significance of model parameters for both the measurement and structural models can be tested by the T -statistics from bootstrapping procedure with 5000 iterations. Given the uncertainty in field measurement and the small sample size (i.e., 25) in the modeling, the lowest significance level for a hypothesis test was set at 0.10 level.

3. Results

3.1. Simple linear relationships for rainfall-runoff-erosion

To demonstrate that there may be an interaction, the first step is to determine the simple main effects. The simple main effects of rainfall and soil on runoff and erosion can be directly recognized by the simple linear regression analyses based on event data in Fig. 3a and b, respectively. On one hand, there appeared a simple main effect of rainfall. High rainfall erosivity generally resulted in higher yields of runoff and sediment than low rainfall erosivity. The regression coefficients were all positive and significantly different from zero ($p < 0.05$). The coefficients of determination (R^2) were all above 0.75 ($p < 0.05$), in which the R^2 ranged from 0.80 to 0.97 in rainfall-runoff regressions (Fig. 3a) and from 0.78 to 0.98 in rainfall-erosion regressions (Fig. 3b). Thus rainfall erosivity had strong explanatory power for the variances in runoff generation (average 88.5%) and soil loss (average 87.8%). On the other hand, there also appeared a simple main effect of soil. Different soil conditions lead to different rates of variation in runoff and erosion with rainfall erosivity. The regression coefficients for rainfall-runoff and rainfall-erosion relationships, namely the potentialities of runoff and erosion are different among soils. The slopes of the fitting lines for rainfall-runoff relationships were ranked as Purple soil (0.070) > Red soil (0.048) > Loess soil (0.027) > Karst soil (0.023) (Fig. 3a). The slopes of the fitting lines for rainfall-erosion relationships were ranked as Loess soil (0.051) > Red soil (0.028) > Purple soil (0.017) > Karst soil (0.013)

(Fig. 3b). Taken together, the unmatched slope rankings between rainfall-runoff and rainfall-erosion regressions on the four soils implied different levels of sediment concentration in different soil conditions. As seen in Fig. 3c, the sediment concentrations were ranked as Loess soil (1.804) > Red soil (0.561) > Karst soil (0.514) > Purple soil (0.238).

3.2. Double-mass curve relationships for rainfall-runoff-erosion

To confirm whether the rainfall-runoff and rainfall-erosion relationships remain the same for all storms, double-mass curve analyses were performed to check the non-linearity. Evident breaks (namely critical points) in the slopes of rainfall-runoff (Fig. 4) and rainfall-erosion curves (Fig. 5) were observed on all soil types. The slope of the rainfall-runoff curve measures the level of runoff induced by unit rainfall effect that reflects the runoff generation potentiality, namely runoff-ability ra . The slope of rainfall-erosion denotes the rate of soil loss caused by unit rainfall effect that represents the soil loss potentiality, i.e. soil erodibility K . The ratio b_n/b_{n-1} for each break was either below 0.80 or above 1.20, indicating the significant change. Thus over 20% variations in potentialities of runoff and erosion after the breaks were identified for all the four soils, indicating that the potentialities of runoff and erosion were significantly affected by the level of rainfall erosivity.

Moreover, the changing patterns of double-mass curves are different among the four soils. With regard to rainfall-runoff curves, moderate decrease (21%) and compelling increase (93%) in the slopes after the break were found on the Loess soil and Purple soil, respectively; and striking decreases (above 50%) in the slopes after the breaks were shown on the Karst soil and Red soil (Fig. 4). As for rainfall-erosion curves, moderate increase (42%) and compelling increase (102%) in the slopes after the break were observed on the Loess soil and Purple soil, respectively; and a strong decrease (58%) in the slope after the break appeared on the Red soil; whereas a complex three stages with two breaks in rainfall-erosion curves were shown on the Karst soil with dramatic increase (540%) and then moderate decrease (42%) in the slopes after the first and then the second break (Fig. 5). These different changing patterns revealed that the effects of rainfall factor on the potentialities of runoff and erosion were substantially controlled by the soil condition.

Different change direction and break position between rainfall-runoff and rainfall-erosion curves caused the varying level of sediment concentration with increasing rainfall erosivity, especially on the Loess soil and Karst soil (Fig. 6). The sediment concentrations for the Loess soil and Karst soil increased to 1.96 and 1.62 times the common level when runoff depth exceeded 29.54 mm and 23.04 mm, respectively. Whereas sediment concentrations for the Purple soil and Red soil were relatively steady with the upgrade of rainfall erosivity. Thus the sediment concentration that reflects the relationship between runoff and erosion had

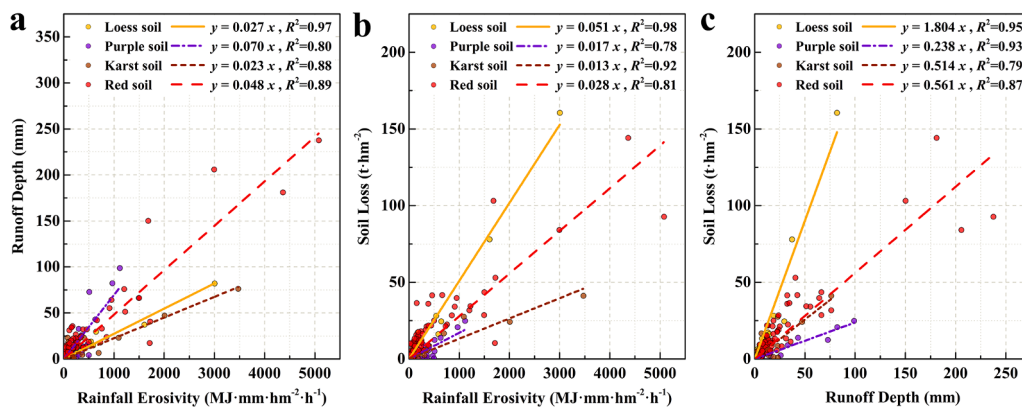


Fig. 3. Relationships between (a) rainfall erosivity and surface runoff, (b) rainfall erosivity and soil loss, (c) surface runoff and soil loss. All the regression coefficients are significantly different from zero at the 0.05 level.

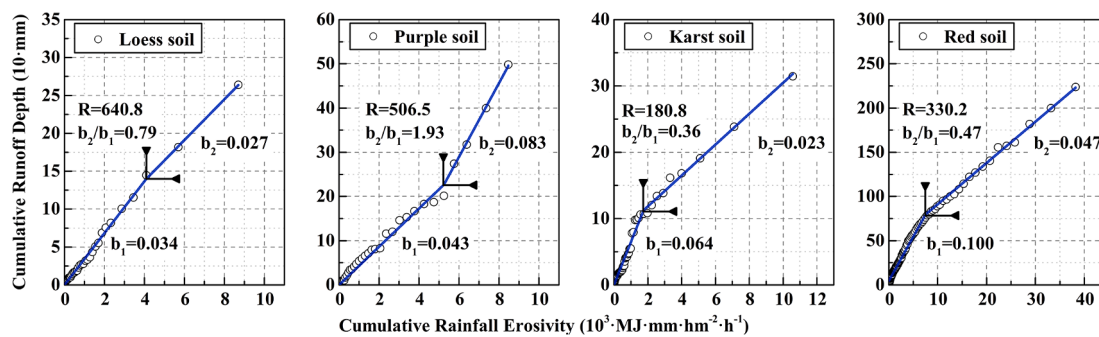


Fig. 4. Double-mass curve analysis of rainfall erosivity and surface runoff. R: rainfall erosivity at the critical point; b_n/b_{n-1} denotes the change degree of the slope.

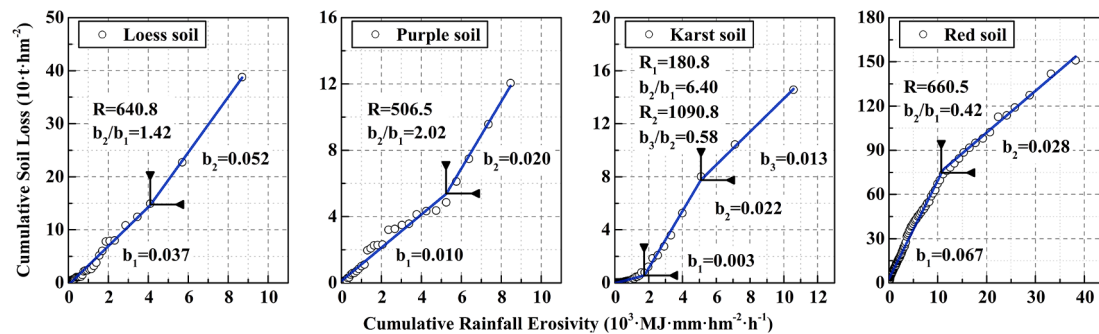


Fig. 5. Double-mass curve analysis of rainfall erosivity and soil loss. R: rainfall erosivity at the critical point; b_n/b_{n-1} denotes the change degree of the slope.

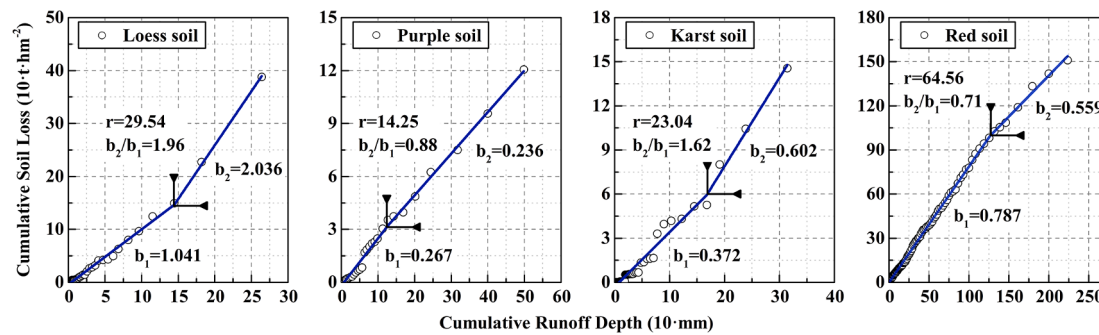


Fig. 6. Double-mass curve analysis of surface runoff and soil loss. r: runoff depth at the critical point; b_n/b_{n-1} denotes the change degree of the slope.

different responses when it comes to different rainfall magnitudes or soil types. And the uncertain relationships between runoff and erosion may be evidence of the complexity of interaction effects of soil and rainfall factors on the hydrological and erosion processes.

3.3. Errors in runoff and erosion predictions

For surface runoff, the ‘predicted’ and ‘measured’ values along the change of rainfall erosivity were plotted in Fig. 7. The NSEs for runoff estimation ranged from 0.71 to 0.95 indicating good prediction efficiency, in which annual prediction outperformed the event prediction. The NRMSEs, namely prediction errors, for runoff estimation ranged from 0.50 to 1.13 with an average of 0.82 for event prediction indicating unacceptable results, fairly higher than the NRMSEs for the annual prediction that ranged from 0.10 to 0.29 with an average of 0.20. In respect of soil type, Purple soil and Karst soil had lower NSEs and higher NRMSEs thus lower prediction accuracy than the cases for Loess soil and Red soil. Regarding the results of MAEs, Loess soil had the lowest magnitude of errors, Red soil had the highest value due to rich rainfall, and Karst soil and Purple soil belonged to the medium level. Overall, the

predictions of surface runoff have better performances on Loess soil and Red soil than that on Purple soil and Karst soil.

Based on the critical points in rainfall-runoff double-mass curve (Fig. 4), more in-depth segmental error analyses of runoff prediction based on rainfall erosivity ranges for different soils are listed in Table 2. Runoff yields on Loess soil, Karst soil, and Red soil were commonly under-predicted for small rainfall events but over-predicted for big storms. On the contrary, runoff yield on Purple soil was majorly over-predicted with an MAE of 5.3 mm for small rainfall events but under-predicted by 36.2% with an MAE of 26.8 mm for big storms over 506.5 EI. These features of error distribution for individual runoff estimation generally agree with the cases for the annual estimation. For instance, runoff yields in the high-rainfall year were under-predicted on Purple soil but over-predicted on Loess soil, Karst soil, and Red soil (Fig. 7).

For soil loss, the comparisons of ‘predicted’ and ‘measured’ values along with increasing rainfall erosivity were shown in Fig. 8. The NRMSEs for event erosion prediction ranged from 0.57 to 0.98 with an average of 0.85 indicating unacceptable erosion prediction errors, in contrast to the low NRMSEs for the annual prediction that ranged from

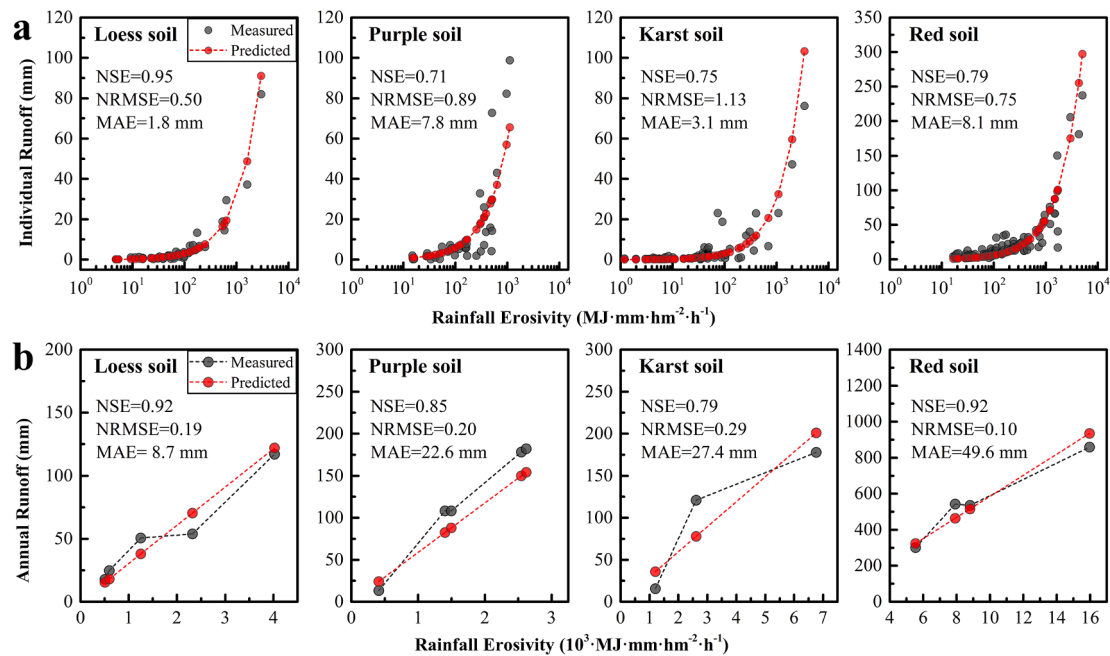


Fig. 7. ‘Predicted’ vs. ‘Measured’ surface runoff on a 20 m slope length and 15° slope gradient plot with different rainfall erosivity regarding (a) individual events and (b) annual values. Runoff prediction equation: $r = R \times ra \times L \times S$; NSE: Nash-Sutcliffe efficiency; NRMSE: normalized root mean square error; MAE: mean absolute error.

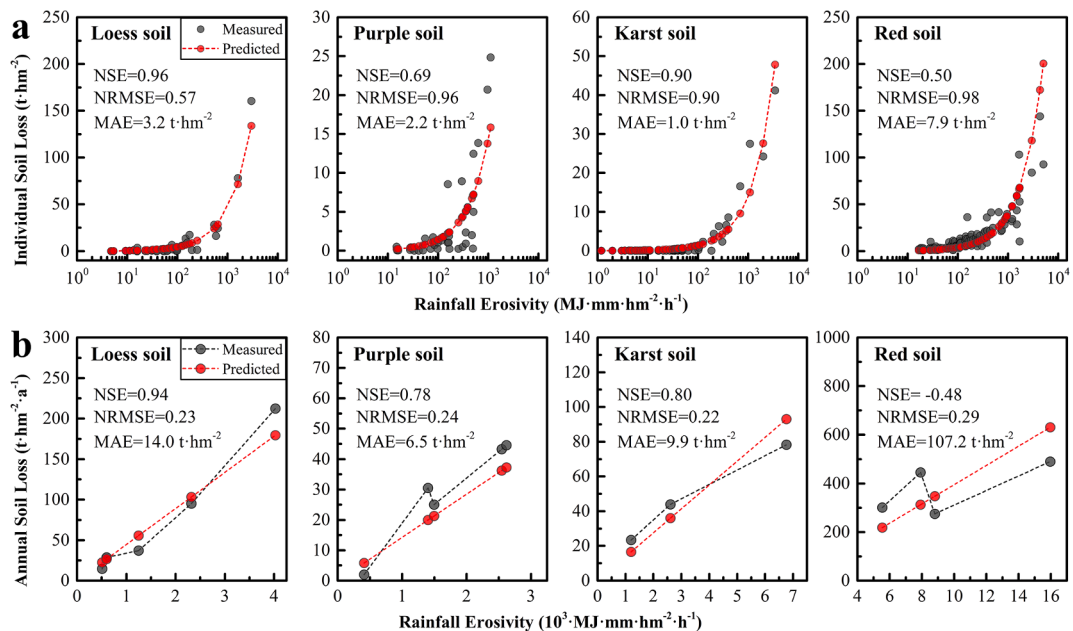


Fig. 8. ‘Predicted’ vs. ‘Measured’ soil loss on a 20 m slope length and 15° slope gradient plot with different rainfall erosivity regarding (a) individual events and (b) annual values. Soil loss prediction equation: $A = R \times K \times L \times S$; NSE: Nash-Sutcliffe efficiency; NRMSE: normalized root mean square error; MAE: mean absolute error.

0.22 to 0.29 with an average of 0.24. Compared to the Loess soil and Karst soil, the Purple soil and Red soil had lower NSEs but higher NRMSEs thus lower prediction accuracy. Especially for annual soil loss prediction on the Red soil, the NSE was a negative value (-0.48) indicating an unacceptable performance that the predictor was less agreeable than the mean observed value. As for the results of MAEs, Red soil had the highest average magnitude of errors, Loess soil belonged to the medium level, and Karst soil and Purple soil had the lowest value. Taken as a whole, both individual and annual estimations of soil loss using USLE had better performance on Loess soil and Karst soil than that on

Purple soil and Red soil.

According to the critical positions in rainfall-erosion double-mass curves (Fig. 5), dissection error analyses of erosion prediction based on rainfall erosivity ranges are presented in Table 3. Largely, soil loss yields on Loess soil and Purple soil tended to be over-predicted in small rainfall events but under-predicted in big storms over 640.8 EI. Whereas soil loss yield on Red soil was mostly under-predicted with an MAE of 4.5 $\text{t} \cdot \text{hm}^{-2}$ for small rainfall events but over-predicted with an MAE of 25.3 $\text{t} \cdot \text{hm}^{-2}$ for big storms over 660.5 EI. Similarly, soil loss yields on Karst soil was over-predicted by 15.3% with an MAE of 5.0 $\text{t} \cdot \text{hm}^{-2}$ for extreme storms

over 1090.8 EI , but majorly under-predicted with an MAE of 4.1 $t \cdot hm^{-2}$ for medium storms and mostly over-predicted with an MAE of 0.3 $t \cdot hm^{-2}$ for light rainfalls $< 180.8 EI$. Combined with the comparison between 'predicted' and 'measured' values of annual erosion, the above segmental features of prediction bias of events erosion estimation generally agree with that of the annual erosion estimation. For instance, soil loss amounts in the high-rainfall year were under-predicted on Loess soil and Purple soil but over-predicted on Karst soil and Red soil (Fig. 8).

3.4. Identification of interaction effects using PLS path modeling

PLS-SEM results of two runoff models (Fig. 9) and two erosion models (Fig. 10) were compared. Stone-Geisser's Q^2 values for the two pairs of models were all above 0.5, suggesting that the two-factor model was predictive whether the interaction factor was incorporated or not. The coefficient of determination (R^2) for the two pairs of models were all above 0.75, indicating substantial predictive accuracy with or without the interaction factor. However, the contribution of interaction effects beyond the simple main effects was substantial in the accuracy improvements for the predictions of runoff and erosion. The R^2 for the

runoff model with interaction term reached 0.952 (Fig. 9a), apparently higher than the 0.872 for the model without interaction (Fig. 9b). A similar trend was observed for erosion models: the R^2 for the model with interaction reached 0.923 (Fig. 10a), higher than the 0.890 for the model without interaction (Fig. 10b). Thus models with interaction consideration could explain more variance in *Annual Runoff* and *Annual Soil Loss*.

Concerning the detection of the interaction effects, both the effect size and regression coefficients were tested (Tables 4). The effect sizes of the *Interaction Effects* were large for both *Annual Runoff* ($f^2 = 1.67$) and *Annual Soil Loss* ($f^2 = 0.93$), indicating that the improvement of R^2 reached a significant level (Henseler and Fassott, 2010), i.e. a practical significance. Plus the statistical significance that the path coefficients of the *Interaction Effects* on *Annual Runoff* ($\beta = -0.274$) and *Annual Soil Loss* ($\beta = -0.169$) were both negative and significantly different from zero ($p < 0.10$). Taken together, these results indicated that the interaction effects imposed practically and statistically significant negative impacts on the predictions of both runoff and erosion.

Regarding the results of the simple main effects, practically and statistically significant main effects of rainfall and soil factors were also

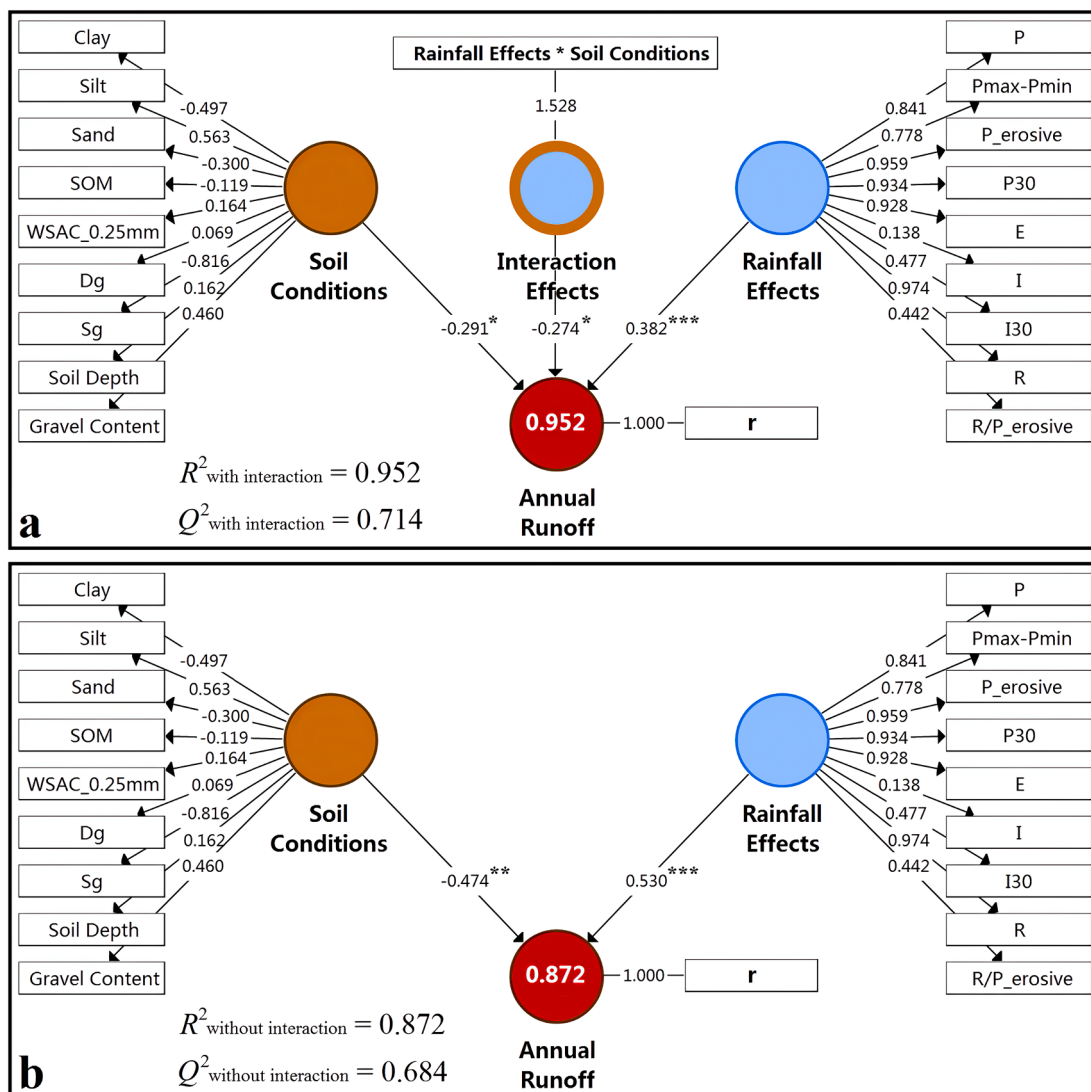


Fig. 9. PLS-SEM results for runoff modelling (a) with interaction and (b) without interaction terms. The numbers on the arrows for indicators are loadings and those for constructs represent the path coefficients. R^2 , coefficient of determination, represents the goodness of fit for the model (the outcome in the red circle). Q^2 is the model's predictive relevance about the endogenous variable. A single asterisk (*), $p < 0.10$; double asterisks (**), $p < 0.05$; triple asterisks (***) $, p < 0.01$; plain entries indicate terms that were not significant in the model. (For interpretation of the references to colour in this figure legend, the reader is referred to the web version of this article.)

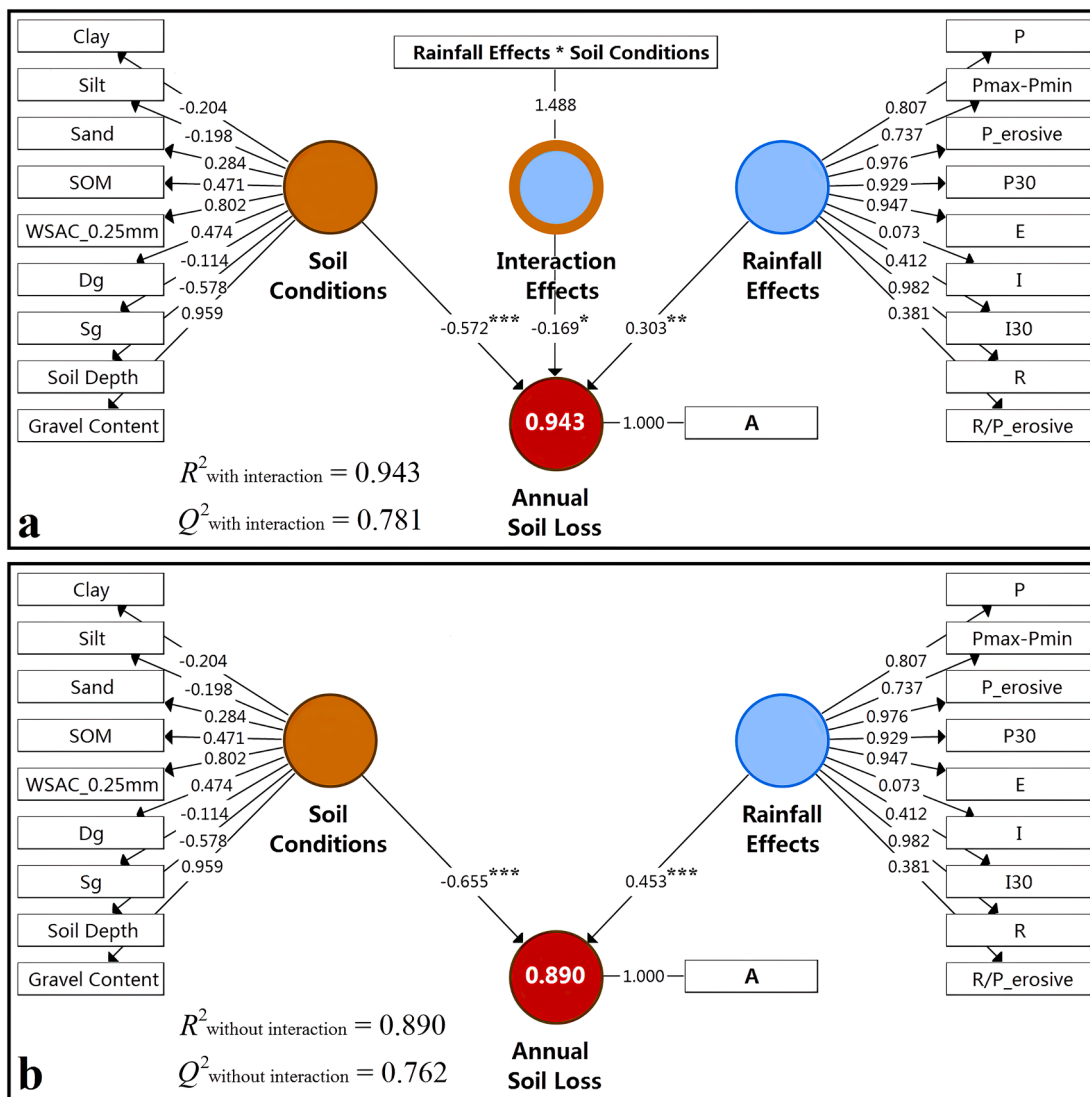


Fig. 10. PLS-SEM results for erosion modelling (a) with interaction and (b) without interaction terms. The numbers on the arrows for indicators are loadings and those for constructs represent the path coefficients. R^2 , coefficient of determination, represents the goodness of fit for the model (the outcome in the red circle). Q^2 is the model's predictive relevance about the endogenous variable. A single asterisk (*), $p < 0.10$; double asterisks (**), $p < 0.05$; triple asterisks (***) $, p < 0.01$; plain entries indicate terms that were not significant in the model. (For interpretation of the references to colour in this figure legend, the reader is referred to the web version of this article.)

verified (Tables 4). Effect sizes for the *Rainfall Effects* and *Soil Conditions* were also rated as large ($f^2 > 0.35$) for both runoff and erosion models, proving practically significant simple main effects from rainfall and soil factors. Moreover, *Rainfall Effects* had a statistically significant and positive path coefficient for *Annual Runoff* ($\beta = 0.382$, $p < 0.01$) as well as *Annual Soil Loss* ($\beta = 0.303$, $p < 0.05$). Contrariwise, *Soil Conditions* had a statistically significant and negative path coefficient for *Annual Runoff* ($\beta = -0.291$, $p < 0.10$) as well as *Annual Soil Loss* ($\beta = -0.572$, $p < 0.01$). By comparing the two path coefficients, we could draw an interesting tendency that the *Annual Runoff* was more sensitive to *Rainfall Effects*, while the *Annual Soil Loss* was more sensitive to *Soil Conditions*. Since significant negative effects of soil factor (i.e. *Soil Conditions*) were tested in both runoff model and erosion model, the specific indication of the *Soil Conditions* in the two models should be identified. In the runoff model, the *Soil Conditions* should indicate soil permeability given the significant positive correlation between *Soil Conditions* and Gravel Content as well as Silt (loadings are 0.460 and 0.563, respectively, $p < 0.10$). In the erosion model, the *Soil Conditions* should denote soil anti-erodibility considering the significant positive correlation between *Soil Conditions* and WSAC_{0.25mm} as well as Gravel

Content (loadings are 0.802 and 0.959, respectively, $p < 0.01$). Thus we defined the soil factor in runoff model as soil permeability while in erosion model as soil anti-erodibility. These results demonstrated that either higher rainfall or lower soil permeability or soil anti-erodibility alone could lead to higher annual yields of runoff and erosion.

Moreover, individual indicator's correlation and reliability to their factor in the models with interaction terms were evaluated (Tables 4). The T-statistics for significance testing of indicator loadings give clues to the correlations between the factor and its indicators. Rainfall indicators that highly denote annual rainfall power, including P, P_{max}-P_{min}, P_{erosive}, P₃₀, E, R, and R/P_{erosive}, were significantly ($p < 0.05$) correlated with the *Rainfall Effects* on both runoff and erosion. Soil indicators that associate with soil permeability, including Sg (Borselli et al., 2009), Silt, and Gravel Content, were significantly ($p < 0.10$) correlated with *Annual Runoff* and that relate to soil erodibility, such as Gravel Content, WSAC_{0.25mm}, Soil Depth, Dg (Shirazi and Boersma, 1984), and SOM, were significantly ($p < 0.05$) correlated with *Annual Soil Loss*. Regarding the indicator reliability, the reliability of individual indicators for *Rainfall Effects* was majorly acceptable either in the runoff model or erosion model. The indicator reliability values of P, P_{max}-P_{min}, P_{erosive},

Table 4

Analysis of model reliability and validity in SEM-PLS modeling with interaction.

Construct	Indicator	Runoff with interaction effects				Erosion with interaction effects			
		Indicator loadings	Indicator reliability	Path coefficient (β)	Effect size (F^2)	Indicator loadings	Indicator reliability	Path coefficient (β)	Effect size (F^2)
Rainfall Effects	P	0.841***	0.707	0.382***	1.26	0.807***	0.651	0.303**	0.48
	$P_{\max} - P_{\min}$	0.778***	0.605			0.737***	0.543		
	P_{erosive}	0.959***	0.920			0.976***	0.953		
	P_{30}	0.934***	0.872			0.929***	0.863		
	E	0.928***	0.861			0.947***	0.897		
	I	0.138	0.019			0.073	0.005		
	I_{30}	0.477**	0.228			0.412**	0.170		
	R	0.974***	0.949			0.982***	0.964		
	R/P_{erosive}	0.442**	0.195			0.381**	0.145		
Soil Conditions	Clay	-0.497	0.247	-0.291*	0.69	-0.204	0.042	-0.572***	2.44
	Silt	0.563*	0.317			-0.198	0.039		
	Sand	-0.300	0.090			0.284	0.081		
	SOM	-0.119	0.014			0.471**	0.222		
	WSAC _{0.25mm}	0.164	0.027			0.802***	0.643		
	Dg	0.069	0.005			0.474**	0.225		
	Sg	-0.816*	0.666			-0.114	0.013		
	Soil Depth	0.162	0.026			-0.578**	0.334		
	Gravel Content	0.460*	0.212			0.959***	0.920		
Interaction Effects	Rainfall Effects * Soil Conditions	1.528***	2.335	-0.274*	1.67	1.488***	2.214	-0.169*	0.93

Note: A single asterisk (*), $p < 0.10$; double asterisks (**), $p < 0.05$; triple asterisks (***) , $p < 0.01$; plain entries indicate terms that were not significant in the model.

P_{30} , E, and R showed to be above 0.4 and thus acceptable, whereas values of I, I_{30} , and R/P_{erosive} were less than 0.4. As for *Soil Conditions*, only the indicator reliability values of Sg in the runoff model and of WSAC_{0.25mm} and Gravel Content in the erosion model were in an acceptable range. In general, the results prove that the constructed interaction models are effective and valid.

4. Discussions

4.1. Simple main effects of rainfall and soil behind linear relationships

The linear regression for rainfall-runoff-erosion relationships on the four soils indicated that both rainfall and soil had strong simple main effects on storm-based runoff generation and soil loss. Previous studies have demonstrated that rainfall is the initial and fundamental driving force to cause the break, detachment, and displacement of soil particles (Wu et al., 2018; Zambon et al., 2021). Thus the main effect of rainfall that determines the magnitude and range of runoff and erosion yields is easy to understand. While the main effect of soil is a complex that integrates the effects of various soil indexes. It determined the potentialities of runoff and erosion that represents the long-term integrated response of soil to a variety of hydrological and erosion processes. Our results showed that the potentialities of both runoff and erosion were different among soils, which may be due to the different combinations of soil intrinsic properties and its external conditions.

Runoff potentiality (i.e. runoff-ability ra) decreased in the order of Purple-Red-Loess-Karst soil (Fig. 3a), which could be attributed to the decreasing soil water holding capacity determined by soil thickness, soil texture, and bedrock permeability. For Purple soil, the thin-bedded silt loam above impermeable sand-shale of the Jurassic Suining Formation could easily reach the saturation point and thus instantly developed productive saturation-excess overland flow (Zhong et al., 2019). For the Karst soil, the thin-bedded clay above fractured limestone bedrock has multiple permeable pathways, such as fissures in the carbonate bedrock (Siemers and Dreybrodt, 1998), cracks in clay soil (Zhu et al., 2018), and rock-soil interfaces (Sohrt et al., 2014). These karstic fracture networks allowed the rapid infiltration of gravity-driven flow or preferential flow (Yang et al., 2016), which resulted in the low potentiality of surface runoff in the shallow karst vadose zone. The Loess soil and Red soil had medium runoff potentialities because the thick soil profile and rich fine particles facilitated the occurrence of the mild infiltration-excess

overland flow; whereas the relatively more clay facilitated the higher runoff potential of Red soil comparing to the Loess soil.

Erosion potentiality (i.e. soil erodibility K) decreased in the order of Loess-Red-Purple-Karst soil (Fig. 3b). This rank is consistent with the rank of soil organic matter (SOM) and water-stable aggregate content (WSAC); and it agrees well with an existing study of sediment yields for different soil types under the same rainfall conditions (Wang et al., 2011). Our statistical analyses showed that the K value had a significant negative correlation with WSAC ($r = -0.989$, $p < 0.05$), insignificant negative correlations with SOM ($r = -0.788$, $p > 0.05$), clay ($r = -0.659$, $p > 0.05$), and rock fragment ($r = -0.880$, $p > 0.05$), and an insignificant positive correlation with soil thickness ($r = 0.916$, $p > 0.05$). These results agree with the findings reported by Liu et al. (2020) on soil aggregates, Fu et al. (2011) on soil thickness, and Niu et al. (2019) on rock fragments. Most notably, the soil aggregate stability was expected to be the critical factor that determined soil erodibility.

4.2. Interaction effects of rainfall and soil behind non-linear relationships

Once the effect of an independent variable is not linear to the dependent variable but depends on the condition of the other independent variable, then the two factors interact (Cox, 1984; Dodge and Commenges, 2006). The USLE-based models assume that soil erodibility K factor is a constant value for a specific soil that is independent of the rainfall erosivity R factor. Early study has clearly pointed out that soil erodibility varies non-uniformly with rainfall erosivity (Morgan, 1983). Our results further suggested that erodibility K is not a definite constant for all storms, but could vary with the level of erosivity R in different patterns among soils; the same for the runoff-ability ra . On one hand, the potentialities of runoff and erosion (i.e. runoff-ability ra and erodibility K) that determined by soil conditions changed with the level of rainfall erosivity with over 20% or even 100% variations, suggesting that the soil effect depended on the rainfall condition. On another hand, the change patterns were different among soils, revealing that the rainfall effect also depended on the soil condition. In the following discussion of the reasons behind these interaction behaviours, we would assess the two aspects for runoff and erosion separately.

The variation of runoff potentiality with the increasing level of rainfall erosivity on the four soils (Fig. 4) could be divided into two groups considering the soil thickness. For thick soils where infiltration-excess overland flow prevails, i.e., the Loess soil (Depth > 200 cm) and

Red soil (Depth > 100 cm), the potentiality of runoff was relatively steady but tended to decrease after a critical point of rainfall erosivity. The decrease was slight on Loess soil (21%) but considerable on Red soil (53%), which may be due to the difference in soil texture (Table 1). Given the depletion of fine particles during a long rainstorm, the surface of granite-derived Red soil with high content of sand (49%) tended to be coarsened with more macro-pores and thus the potentiality of runoff decreased (Mamedov et al., 2001). While this phenomenon could hardly happen on the Loess soil with very low content of sand (14.5%). As for the soils with very limited soil depth, the variations of runoff potentiality were more evident and the change direction was determined by the permeability of bedrock. For thin soils above impermeable bedrock, such as the Purple soil (Depth = 40 cm), the potentiality of runoff increased by 93% after the rainfall erosivity exceeded 506.5 EI , which may be due to that the productive saturation-excess overland flow was initiated by the saturation of the shallow soil layer (Ferreira et al., 2016). However, this trend was reversed for the same shallow Karst soil (Depth = 21 cm) and its runoff-ability ra decreased by 64% once the rainfall exceeded 180.8 EI . This paradox was likely due to the rich fissures in the fractured-karstified limestone underlying the thin soil (Macpherson, 1996). Once the saturation point was reached within the thin soil, excess water would quickly flow through the paths in fractured bedrocks to groundwater (Ford and Williams, 2013). Thus the subsequent runoff generation did not change to saturation-excess but an even more weak infiltration-excess flow.

The variation of erosion potentiality with the increasing level of rainfall erosivity on the four soils (Fig. 5) could be divided into two groups. One is for the Purple soil and Red soil that the variation of erodibility K coincided with that of runoff-ability ra . For the Purple soil, the saturation of the shallow soil layer (Depth = 40 cm) above the impermeable bedrock (sand-shale) could initiate the shift of hydrological process from infiltration-excess to saturation-excess runoff generation, but also induce the shift of erosion process from rainfall-driven to runoff-driven transport and thus the increase in sediment transportation. For the sandy clay loam Red soil (Sand = 49.0%, Clay = 26.2%, Silt = 24.8%), the coarsening of soil surface could facilitate the infiltration, but also reduce the capacity of flow to cause erosion and increase the resistance of soil surface (Descroix et al., 2001). Another group is for the Loess soil and Karst soil that the variation of erodibility K did not coincide with that of runoff-ability ra . For the fine-textured Loess soil (Silt = 70.6%, Clay = 14.9%) that lacks of aggregation (WSAC = 23.4%), sealing and crusting were prone to form by raindrop impact; however, once the power of rainfall exceeded the resistance of the crusts, rills were likely to develop on the exposed soil (Slattery and Bryan, 1992) and the subsequent erosion processes tended to transform from inter-rill to rill erosion (Moore and Singer, 1990). This transformation induced by the failure of soil crusts has been expected to cause a decrease in the runoff potentiality (Moss and Watson, 1991), an increase in the erosion potentiality (He et al., 2017), and higher sediment concentration (Sun et al., 2019), which agrees well with our results (Figs. 4–6). For the Karst soil, the runoff-ability ra decreased but the erodibility K increased when the light rainfall upgraded to moderate rainfall over 180.8 EI . The increase in K may relate to the characteristic of clay soil that is hardly erodible in gentle rainfall but intensively eroded in intensive rainfall (Wu et al., 2017b). While the decrease of runoff potentiality was expected to have a prolonged effect on the erosion potentiality considering the decrease of K when the rainfall exceeded 1090.8 EI (Figs. 4, 5).

From the above analyses, it seemed that different combinations of intrinsic properties (e.g. soil texture and aggregation) and external conditions (e.g. soil depth and bedrock permeability) of soil could trigger different shifts of hydrological and erosion processes during rainfall. In which, the intrinsic properties (sandy, fine-textured and poor aggregation) associated with the change of soil surface (coarsening, crusting or decrusting), the external conditions (thin soil above impermeable or fractured bedrock) determined the change of soil infiltration

(decelerate or accelerate) when the soil was saturated.

4.3. Interaction effects of rainfall and soil in PLS path modeling

A previous study suggested that the erosion model incorporating the interaction of factors may have more convincing outputs than the model arranging factors in isolation (Beven and Brazier, 2011). Our study further proves that factoring in the interaction effects is expected to substantially improve the model performance in the predictions of runoff and erosion. The PLS path modeling results showed that the model could still have high predictive capability even if excluded the interaction factor. However, the model with interaction consideration could substantially improve the prediction accuracy. The addition of the interaction factor contributed 9.2% and 6.0% increase in the coefficient of determination (R^2) for the prediction of annual runoff and erosion, respectively. The improvements reached significant levels because the effect sizes (f^2) of the interaction terms were large for both runoff and erosion. Besides, significant path coefficient (β) of the interaction factor further support the hypothesis on the existence of significant interaction effects.

Notably, the negative effects ($\beta < 0$) of the interaction of rainfall and soil factors that exerted on annual runoff and erosion need to be clarified. The simple interpretation is that the more interaction effects, the less runoff generation and soil loss. The models in Fig. 9a and Fig. 10a could be specified as:

$$\begin{aligned} \text{Surface Runoff} = & 0.382 * \text{Rainfall Effects} - 0.291 * \text{Soil Permeability} \\ & - 0.274 * \text{Interaction Effects} + e \end{aligned} \quad (8)$$

$$\begin{aligned} \text{Soil Loss} = & 0.303 * \text{Rainfall Effects} - 0.572 * \text{Soil Anti-erodibility} \\ & - 0.169 * \text{Interaction Effects} + e \end{aligned} \quad (9)$$

Where e is the measurement error; *Interaction Effects* for Eq. (8) refers to *Rainfall Effects* \times *Soil Permeability* and for Eq. 9 represents *Rainfall Effects* \times *Soil Anti-erodibility*. It is easy to understand that either higher rainfall or lower soil permeability or soil anti-erodibility alone could lead to higher annual yields of runoff and erosion. However, how to explain the higher rainfall and soil permeability (namely the higher *Rainfall Effects* \times *Soil Permeability*) the lesser runoff, and the higher rainfall and soil anti-erodibility (namely the higher *Rainfall Effects* \times *Soil Anti-erodibility*) the lesser erosion?

Concerning the reason for the negative interaction phenomenon, there might be some clues in the variations of runoff and erosion potentialities on the four soils we have mentioned above. For example, the results on the Karst soil fit the case that the higher rainfall and soil permeability the lesser runoff potentiality. As shown in Fig. 4, the runoff potentiality of the Karst soil decreased by 64% once the rainfall exceeded 180.8 EI . Our regression analysis of data on the Karst soil showed that the erosivity from one millimeter of rainfall is 4.91 EI in a rainfall of 180.8 EI , thus the corresponding rainfall amount was about 36.8 mm. Our previous study showed that the volumetric soil water content of the Karst soil was 22% for the antecedent dry condition and 40% for the saturated soil condition (Yang et al., 2021). Thus the rainfall amount that caused saturation should be about 18% of the 21 cm thickness, i.e. 37.8 mm, very close to the 36.8 mm rainfall of 180.8 EI . Obviously, the decrease in the runoff potentiality once the rainfall exceeded 180.8 EI were highly likely to associate with the saturation of the Karst soil. Once the thin Karst soil was saturated, the quick paths in the underlying fractured bedrocks accelerated the infiltration, in accord with the feature of higher rainfall and higher soil permeability. A similar feature could be found on Red soil and Loess soil since the surface coarsening and decrusting could facilitate the infiltration (Liao et al., 2019; Ncizah and Wakindiki, 2015). Regarding the negative path coefficient of interaction effects, the result of the Red soil fits the case that the higher rainfall and soil anti-erodibility the lesser erosion. As seen in Fig. 5, the

erosion potentiality on the Red soil decreased by 53% once the rainfall exceeded 660.5 EI . The coarsening of soil surface on the sandy clay loam could increase the resistance of surface to erosion, in line with the feature of the higher rainfall and higher soil anti-erodibility. A similar feature could be found on the karst soil because the decrease of runoff had the same effect as the increasing soil anti-erodibility. Beyond the above examples, the feature that the higher rainfall and lower soil permeability the more runoff could be found on the thin Purple soil above impermeable bedrock; the feature that the higher rainfall and lower soil anti-erodibility the more erosion could be found on the crust-prone Loess soil. All these coincidences implied that once the rainfall exceeded a critical point that the soil conditions were substantially changed, the subsequent potentialities of runoff and erosion would be greatly changed and thus determined the long-term outcome. From the above, it seemed that the negative interaction was embodied in the variations of runoff and erosion potentialities for a specific soil during large rainfall and its effect could be projected to a long-term result. This may explain the negative interaction in the PLS path modeling that the higher rainfall and permeability the lesser annual runoff, and the higher rainfall and anti-erodibility the lesser annual erosion.

4.4. Prediction uncertainties induced by the interaction effects

There exists a general tendency for over-prediction of small events and under-prediction of large events in respect of runoff and erosion predictions. This well-known prediction bias has been found in the applications of many hydrological and erosion models, such as the USLE (Risse et al., 1993), RUSLE (Rapp, 1994), Water Erosion Prediction Project (WEPP) (Ghidley et al., 1995; Zhang et al., 1996), Soil and Water Assessment Tool (SWAT) (Wolkerstorfer and Strauss, 2004), and Annualized Agricultural Non-Point Source Pollution Model (AnnAGNPS) (Polyakov et al., 2007). Some researchers attributed this tendency to the result of the inherent characteristic of the erosion model that can hardly capture the unpredictable ‘natural variation’ (Nearing, 1998; Tiwari et al., 2000). While Kinnell (2003) explained the overestimation of small events through the soil properties. He noted that the overestimation of small events tends to occur on the soil that has a high capacity to infiltrate rainfall, and the degree of overestimation increases with the capacity of the soil to infiltrate rainfall. That is, the higher soil permeability, the more overestimations of runoff and erosion in small events. This conclusion agrees well with our results, and we would further provide deeper insight into the reason behind the prediction bias tendency in the following discussion.

We could speculate from the study of Kinnell (2003) that the overestimation of small events would be a big problem for soils with high inherent permeability, and the underestimation of small events may be a considerable issue for soils with low inherent permeability. Our error evaluation for the prediction cases that ignore the nonlinearities from the interaction effects could support this speculation. The results for runoff (Table 2) showed that about 75% of small events were overpredicted for Purple soil that has high inherent permeability; while 70% of small events were also under-predicted for Karst soil that has low inherent permeability due to the high content of clay. The corresponding results for erosion (Table 3) showed that about 77% of small erosion events were over-predicted for Purple soil with high inherent permeability, in accord with its result for runoff. However, we found that about 95% of small erosion events were over-predicted for Karst soil with low inherent permeability, which may be due to the high anti-erodibility of clay. This contradiction indicated that soil anti-erodibility rather than soil permeability should be the main index that implies the prediction bias of small erosion events. Thus the runoff overestimation of small events tended to occur on soil with high permeability (e.g. coarse-textured Purple soil), while the erosion overestimation of small events tended to occur on soil with high anti-erodibility (e.g. Purple soil and Karst soil with high aggregation and gravel). By the vice versa principle, the underestimations of runoff and erosion in small events are expected

to occur on soil with low permeability (e.g. Red soil and Karst soil with high clay) and low anti-erodibility (e.g. Red soil with low aggregation), respectively. The above examples in the parentheses are all the evidence from our results to support the corresponding reasoning results. However, there is an extraordinary case that the Loess soil with high permeability and low anti-erodibility tended to underestimate runoff and overestimate erosion of small events. This can be attributed to the crust-prone feature of the Loess soil. Because the soil crusts can reduce infiltration and produce an equivalent effect of low permeability, but also protect soil and result in a high anti-erodibility. Thus, when we need to forecast the prediction bias for small events or for the period with more frequent small events, the intrinsic permeability and anti-erodibility of soil are the foremost diagnostic indicators, and the typical change of soil surface in small events, such as sealing and crusting, should also be taken into consideration.

Following the clue of the above analysis for the small events, we may further into the explanation for prediction bias of large events. Similar to the small events, the capacity of the soil to produce runoff or resist erosion is expected to indicate the prediction bias of runoff or erosion in large events, respectively. But unlike the small events that mainly focus on the intrinsic properties of soil, the consideration for large events should also take into account the external conditions associated with soil such as the soil crust, soil depth, bedrock permeability, gravel or rock involvement, among others. Our preceding analyses indicated that these features could trigger the changes of hydrological and erosion processes when the soil layer was saturated or the soil surface changed evidently during a large rainfall. That is, the soil conditions that imply the prediction bias of large events were not unvarying but would change after a critical point of rainfall. Thus, the change of infiltration rate of the whole vadose zone (the layer of soil and rock) could imply the runoff prediction bias of large events; the variation of anti-erodibility of the land surface (including crust and soil) may indicate the erosion prediction bias of large events. In which, the increase (higher) and decrease (lower) are expected to denote the overestimation and underestimate. Our segmental error analyses on the four soils can exactly support the above assumption. Regarding the runoff prediction (Table 2), the overestimation of large events that occurred on the Loess soil, Karst soil, and Red soil agrees with the increased infiltration due to the destruction of crusts, the involvement of fractured bedrock underlying thin soil, and the surface coarsening process, respectively. The runoff underestimation of large events that occurred on the Purple soil echoes with the decreased infiltration due to the saturation of thin soil above impermeable bedrock. As for the erosion prediction (Table 3), the overestimation of large events that occurred on the Red soil and Karst soil agrees with the increased anti-erodibility due to the coarsen surface and the increased infiltration due to the saturation of thin soil above fractured bedrock, respectively. The erosion underestimation of large events occurred on the Loess soil and Purple soil accords with the decreased anti-erodibility due to decrusting and the decreased infiltration due to the saturation of thin soil above fractured bedrock, respectively.

From the above, we found that the prediction bias of small events or large events was not an inherent mathematical phenomenon that can hardly explain, but a result of interaction between rainfall and soil that can predict. The prediction bias of small events could be estimated with soil intrinsic permeability and anti-erodibility; and the prediction bias of large events associated with the changes in the infiltration of the whole vadose zone and anti-erodibility of the land surface.

Apart from the segmental prediction bias for small and large events, the reason behind the overall prediction bias should also be explained. Previous studies have suggested that USLE (Risse et al., 1993; Meinen and Robinson, 2021) and WEPP (Ghidley et al., 1995; Zhang et al., 1996) have general over-prediction performances in the estimations of annual runoff and erosion. The negative path coefficients of interaction effects of rainfall and soil factors in our PLS path models may explain the general over-prediction performance of these models without interaction terms. Compared to the model excluding interaction term, the

model with interaction is expected to predict the runoff and erosion with values that closer to the reality. In Eqs. (8) and (9), the *Interaction Effects* were expressed with *Rainfall Effects* \times *Soil Permeability* and *Rainfall Effects* \times *Soil Anti-erodibility* for annual runoff and erosion modeling, respectively. Thus, if the *Rainfall Effects* have no change or difference, the higher *Soil Permeability* the larger *Interaction Effects* for runoff modeling, and the higher *Soil Anti-erodibility* the larger *Interaction Effects* for erosion modeling. As shown in Eqs. (8) and (9), the larger *Interaction Effects* that have negative regression coefficients ($\beta < 0$), the larger overestimations if excluding the *Interaction Effects* in the model with interaction term. That's to say, excluding the interaction effects from the models with interaction is expected to cause overestimations of runoff and erosion. This may explain the overall overestimation phenomena in the existing models without interaction terms. According to the above analyses, *Soil Permeability* means the intrinsic soil permeability for small events while the infiltration of the whole vadose zone for large events; and *Soil Anti-erodibility* denotes the intrinsic soil anti-erodibility for small events while the anti-erodibility of land surface for large events. Thus, when the *Interaction Effects* is factored out, more overestimations of runoff and erosion tend to occur on the soil with high permeability and anti-erodibility, respectively, or the soil with evident increased infiltration and anti-erodibility during large rainfall, respectively. These analyses agree well with the above speculations about prediction bias and thus prove its validity.

5. Conclusions

This study provides robust evidence to support the hypothesis that the interaction effects of rainfall and soil factors exist in the hydrological and erosion processes and thus induce considerable uncertainties in the prediction. The interaction effects were reflected in the non-linearities of rainfall-runoff-erosion relationships, namely the variations of runoff and erosion potentialities for a specific soil during large rainfall. The potentialities of runoff and erosion were determined by the combination of soil intrinsic properties and its external conditions, namely the soil factor. However, the potentialities of both runoff and erosion were not constants for a specific soil but varied with the level of rainfall erosivity in different patterns among soils, indicating the mutual interactions between rainfall and soil factors. The interaction between rainfall and soil is essentially a result of comprehensive effects of rainfall and the whole vadose zone or geological substrate, especially for the region with thin soil. Our PLS path modeling for annual runoff and erosion indicated that the interaction effects of rainfall and soil factors were significant negative ($\beta < 0, p < 0.10$). The negative interaction factors have multi-fold implications. First, runoff and erosion tend to be over-predicted if excluding the interaction factors from the model frame, which agrees with the general overestimation performance of existing models. Second, the higher the soil permeability and anti-erodibility, the more the overestimations on runoff and erosion, respectively. Third, the soil loss from steep slopes still tends to be over-predicted even though the *S* factor has been calibrated, indicating the existing topographic calibration can hardly eliminate the prediction uncertainty from the interaction effects. Moreover, the prediction bias for small events or large events was found predictable and rooted in the interaction between rainfall and soil. This work evidences the importance of factoring in the interaction effects, and the results provide references for the mechanisms behind the non-linearity and the prediction bias in runoff and erosion estimations.

Declaration of Competing Interest

The authors declare that they have no known competing financial interests or personal relationships that could have appeared to influence the work reported in this paper.

Acknowledgements

This study was supported by the National Natural Science Foundation of China (41730748) and the National Key Research and Development Project of China (2016YFC0503705). No conflicts of interest exist in the submission of this manuscript. The authors would like to thank Prof. Yun Xie for providing spatial data of rainfall erosivity in Fig. 1 from the project National Soil Erosion Dynamic monitoring of China (2018–2022).

References

- Aleweli, C., Borrelli, P., Meusburger, K., Panagos, P., 2019. Using the USLE: Chances, challenges and limitations of soil erosion modelling. *Int. Water Conserv. Res.* 7 (3), 203–225.
- Benavidez, R., Jackson, B., Maxwell, D., Norton, K., 2018. A review of the (Revised) Universal Soil Loss Equation ((R)USLE): With a view to increasing its global applicability and improving soil loss estimates. *Hydrol. Earth Syst. Sci.* 22 (11), 6059–6086.
- Beven, K.J., Brazier, R.E., 2011. Dealing with uncertainty in erosion model predictions. In: Morgan, R.P.C., Nearing, M.A. (Eds.), *Handbook of erosion modelling*. Wiley Online Library, pp. 52–79.
- Borselli, L., Cassi, P., Sanchis, P.S., 2009. Soil erodibility assessment for applications at watershed scale. In: Costantini, E. (Ed.), *Manual of methods for soil and land evaluation*. CRC Press, Enfield, NH, USA, pp. 98–115.
- Borselli, L., Torri, D., Poesen, J., Iaquinta, P., 2012. A robust algorithm for estimating soil erodibility in different climates. *CATENA* 97, 85–94.
- Boßow-Thies, S., Albers, S., 2010. Application of PLS in marketing: content strategies on the internet. In: *Handbook of Partial Least Squares*. Springer, pp. 589–604.
- Brown, L., Foster, G., 1987. Storm erosivity using idealized intensity distributions. *Trans. ASAE* 30 (2), 379–386.
- Cebecauer, T., Hoferka, J., 2008. The consequences of land-cover changes on soil erosion distribution in Slovakia. *Geomorphology* 98 (3), 187–198.
- Chamizo, S., Cantón, Y., Rodríguez-Caballero, E., Domingo, F., Escudero, A., 2012. Runoff at contrasting scales in a semiarid ecosystem: A complex balance between biological soil crust features and rainfall characteristics. *J. Hydrol.* 452–453, 130–138.
- Chin, W.W., 2010. How to write up and report PLS analyses. *Handbook of partial least squares*. Springer, pp. 655–690.
- Cohen, J., 1998. Statistical power analysis for the behavioral sciences. Lawrence Erlbaum Associates, New York, USA.
- Cox, D.R., 1984. Interaction. *Int. Stat. Rev.* 52 (1), 1–31.
- Daggupati, P., Deb, D., Srinivasan, R., Yeganathan, D., Mehta, V.M., Rosenberg, N.J., 2016. Large-scale fine-resolution hydrological modeling using parameter regionalization in the Missouri River Basin. *JAWRA J. Am. Water Resour. Assoc.* 52 (3), 648–666.
- Descroix, L., Viramontes, D., Vauclin, M., Barrios, J.L.G., Esteves, M., 2001. Influence of soil surface features and vegetation on runoff and erosion in the Western Sierra Madre (Durango, Northwest Mexico). *Catena* 43 (2), 115–135.
- Dodge, Y., Commenges, D., 2006. *The Oxford dictionary of statistical terms*. Oxford University Press, New York, USA.
- El Kateb, H., Zhang, H., Zhang, P., Mosandl, R., 2013. Soil erosion and surface runoff on different vegetation covers and slope gradients: A field experiment in Southern Shaanxi Province, China. *Catena* 105, 1–10.
- Estrada-Carmona, N., Harper, E.B., DeClerck, F., Fremier, A.K., 2017. Quantifying model uncertainty to improve watershed-level ecosystem service quantification: a global sensitivity analysis of the RUSLE. *Int. J. Biodivers. Sci., Ecosyst. Serv. Manage.* 13 (1), 40–50.
- FAO, IIASA, ISRIC, ISSCAS, JRC, 2012. Harmonized world soil database (version 1.2). FAO, Rome, Italy and IIASA, Laxenburg, Austria.
- Fan, Y., Chen, J., Shirkey, G., John, R., Wu, S.R., Park, H., Shao, C., 2016. Applications of structural equation modeling (SEM) in ecological studies: an updated review. *Ecol. Processes* 5 (1), 19.
- Ferreira, C.S.S., Walsh, R.P.D., Shakesby, R.A., Keizer, J.J., Soares, D., González-Peláez, O., Coelho, C.O.A., Ferreira, A.J.D., 2016. Differences in overland flow, hydrophobicity and soil moisture dynamics between Mediterranean woodland types in a peri-urban catchment in Portugal. *J. Hydrol.* 533, 473–485.
- Ford, D., Williams, P.D., 2013. Karst hydrogeology and geomorphology. John Wiley & Sons.
- Fox, D., Bryan, R.B., 1992. Influence of a polyacrylamide soil conditioner on runoff generation and soil erosion: Field tests in Baringo District, Kenya. *Soil Technol.* 5 (2), 101–119.
- Fu, Z., Li, Z., Cai, C., Shi, Z., Xu, Q., Wang, X., 2011. Soil thickness effect on hydrological and erosion characteristics under sloping lands: A hydropedological perspective. *Geoderma* 167–168, 41–53.
- Ghidye, F., Alberts, E.E., Kramer, L.A., 1995. Comparison of runoff and soil loss predictions from the WEPP hillslope model to measured values for eight cropping and management treatments. *Am. Soc. Agric. Eng. Paper* (95–2383).
- Grace, J.B., 2006. *Structural equation modeling and natural systems*. Cambridge University Press.
- Gu, S.X., 2004. The research on purple soil erosion characteristics and rate of permissible erosion. Southwest Agricultural University, Chongqing, China.

- He, J.J., Sun, L.Y., Gong, H.I., Cai, Q.G., 2017. Laboratory studies on the influence of rainfall pattern on rill erosion and its runoff and sediment characteristics. *Land Degrad. Dev.*, 28(5): 1615–1625.
- Hair Jr, J.F., Hult, G.T.M., Ringle, C.M., Sarstedt, M., 2016. A primer on partial least squares structural equation modeling (PLS-SEM). Sage Publications, Thousand Oaks, CA, USA.
- He, X., 2007. Spatial rule of the soil erosion for the ecological management of the karst regions-A case study of Qingzen, Bijie, Zunyi, Yanhe of Guizhou province. Guizhou Normal University, Guiyang, China.
- Henseler, J., Fassott, G., 2010. Testing Moderating Effects in PLS Path Models: An Illustration of Available Procedures. In: Esposito Vinzi, V., Chin, W.W., Henseler, J., Wang, H. (Eds.), *Handbook of Partial Least Squares: Concepts, Methods and Applications*. Springer, Berlin, Heidelberg, pp. 713–735.
- Hsu, S.H., Chen, W.H., Hsieh, M.J., 2006. Robustness testing of PLS, LISREL, EQS and ANN-based SEM for measuring customer satisfaction. *Total Qual. Manag. Business Excell.* 17 (3), 355–372.
- Hua, T., Zhao, W., Liu, Y., Liu, Y., 2019. Influencing factors and their interactions of water erosion based on yearly and monthly scale analysis: A case study in the Yellow River basin of China. *Nat. Hazards Earth Syst. Sci. Discuss.* 2019, 1–22.
- Hulland, J., 1999. Use of partial least squares (PLS) in strategic management research: A review of four recent studies. *Strat. Manage. J.* 20 (2), 195–204.
- Issa, O.M., Valentini, C., Rajot, J.L., Cerdan, O., Desprats, J.F., Bouchet, T., 2011. Runoff generation fostered by physical and biological crusts in semi-arid sandy soils. *Geoderma* 167–168, 22–29.
- Ki Tiwari, A., M. Risso, L., A Nearing, M., 2000. Evaluation of Wepp and its comparison with USLE and Rusle. *Trans. ASAE*, 43(5): 1129–1135.
- Jiang, N., Shi, D.M., Jiang, G.Y., Song, G., Si, C.J., Ye, Q., 2020. Effects of soil erosion on physical and mechanical properties of cultivated layer of purple soil slope farmland. *Sci. Agric. Sin.* 53 (9), 1845–1859.
- Ke, Q.H., Zhang, K.L., 2021. Patterns of runoff and erosion on bare slopes in different climate zones. *Catena* 198, 105069.
- Kinnell, P.I.A., 2003. Event erosivity factor and errors in erosion predictions by some empirical models. *Soil Res.* 41 (5), 991–1003.
- Le Bissonnais, Y., Renaux, B., Delouche, H., 1995. Interactions between soil properties and moisture content in crust formation, runoff and interrill erosion from tilled loess soils. *Catena* 25 (1–4), 33–46.
- Limayem, M., Hirt, S.G., Chin, W.W., 2001. Intention does not always matter: the contingent role of habit on IT usage behavior. The 9th European Conference on Information Systems, Global Co-Operation in the New Millennium. ECIS, Bled, Slovenia, pp. 274–286.
- Liu, B., Nearing, M., Shi, P., Jia, Z., 2000. Slope length effects on soil loss for steep slopes. *Soil Sci. Soc. Am. J.* 64 (5), 1759–1763.
- Liao, Y.S., Yuan, Z.J., Zhuo, M.N., Huang, B., Nie, X.D., Xie, Z.Y., Tang, C.Y., Li, D.Q., 2019. Coupling effects of erosion and surface roughness on colluvial deposits under continuous rainfall. *Soil Tillage Res.* 191, 98–107.
- Liu, M., Han, G., Li, X., Zhang, S., Zhou, W., Zhang, Q., 2020. Effects of soil properties on K factor in the granite and limestone regions of China. *Int. J. Environ. Res. Public Health* 17 (3), 801.
- Liu, B.Y., Nearing, M.A., Risso, L.M., 1994. Slope gradient effects on soil loss for steep slopes. *Trans. ASAE* 37 (6), 1835–1840.
- Liu, B.Y., Zhang, K.L., Xie, Y., 2002. An Empirical Soil Loss Equation, Proceedings of 12th ISCO Conference, II. Process of soil Erosion and Its Environment Effect. Tsinghua University Press, Beijing, pp. 21–25.
- Macpherson, G.L., 1996. Hydrogeology of thin limestones: the Konza Prairie long-term ecological research site, Northeastern Kansas. *J. Hydrol.* 186 (1–4), 191–228.
- Mamedov, A.I., Levy, G.J., Shainberg, I., Letey, J., 2001. Wetting rate, sodicity, and soil texture effects on infiltration rate and runoff. *Soil Res.* 39 (6), 1293–1305.
- Meinen, B.U., Robinson, D.T., 2021. Agricultural erosion modelling: Evaluating USLE and WEPP field-scale erosion estimates using UAV time-series data. *Environ. Model. Softw.* 137, 104962.
- Moore, D.C., Singer, M.J., 1990. Crust formation effects on soil erosion processes. *Soil Sci. Soc. Am. J.* 54 (4), 1117–1123.
- Morgan, C., 1983. The non-independence of rainfall erosivity and soil erodibility. *Earth Surf. Process. Landforms* 8 (4), 323–338.
- Moss, A.J., Watson, C.L., 1991. Rain impact soil crust. III. Effects of continuous and flawed crusts on infiltration, and the ability of plant covers to maintain crustal flaws. *Soil Res.* 29 (2), 311–330.
- Ncizah, A.D., Wakindiki, I.I.C., 2015. Soil sealing and crusting effects on infiltration rate: a critical review of shortfalls in prediction models and solutions. *Arch. Agron. Soil Sci.* 61 (9), 1211–1230.
- Nearing, M.A., 1998. Why soil erosion models over-predict small soil losses and under-predict large soil losses. *CATENA* 32 (1), 15–22.
- Nishigaki, T., Sugihara, S., Kilasara, M., Funakawa, S., 2017. Surface Runoff Generation and Soil Loss Under Different Soil and Rainfall Properties in the Uluguru Mountains, Tanzania. *Land Degrad. Dev.* 28 (1), 283–293.
- Niu, Y., Gao, Z., Li, Y., Luo, K., 2019. Effect of rock fragment content on erosion processes of disturbed soil accumulation under field scouring conditions. *J. Soils Sediments* 19 (4), 1708–1723.
- Parsons, A.J., 2019. How reliable are our methods for estimating soil erosion by water? *Sci. Total Environ.* 676, 215–221.
- Pimentel, D., 2006. Soil erosion: a food and environmental threat. *Environ., Dev. Sustain.* 8 (1), 119–137.
- Polyakov, V., Fares, A., Kubo, D., Jacobi, J., Smith, C., 2007. Evaluation of a non-point source pollution model, AnnAGNPS, in a tropical watershed. *Environ. Model. Softw.* 22 (11), 1617–1627.
- Rapp, J.F., 1994. Error assessment of the revised universal soil loss equation using natural runoff plot data. The University of Arizona, Tucson, AZ, USA.
- Raza, A., Ahrends, H., Habib-Ur-Rahman, M., Gaiser, T., 2021. Modeling approaches to assess soil erosion by water at the field scale with special emphasis on heterogeneity of soils and crops. *Land* 10 (4), 422.
- Risse, L.M., Nearing, M.A., Lafren, J.M., Nicks, A.D., 1993. Error assessment in the universal soil loss equation. *Soil Sci. Soc. Am. J.* 57 (3), 825–833.
- Roose, E., 1996. Wischmeier and Smith's Empirical Soil Loss Model (USLE) in Chapter 5. Sheet erosion: the initial phase of water erosion. In: Roose, E. (Ed.), *Land husbandry: Components and strategy*. FAO, Rome.
- Ruan, F.S., Zhou, F.J., Nie, B.J., Wu, X.H., Lin, W.L., Chen, M.H., Wu, X.H., Shi, Y.Z., Xu, J.J., 1995. Study on anti-erosion characteristics of granite weathering crust. I. Physical characteristics of granite weathering crust. *Subtrop. Soil Water Conserv.* 4, 37–42.
- Sheng, H., Cai, Q.G., Sun, L.Y., 2016. Impacts of loessial texture on slope erosion. *J. Soil Water Conserv.* 30 (1), 31–35.
- Shirazi, M.A., Boersma, L., 1984. A unifying quantitative analysis of soil texture. *Soil Sci. Soc. Am. J.* 48 (1), 142–147.
- Siemers, J., Dreybrodt, W., 1998. Early development of Karst aquifers on percolation networks of fractures in limestone. *Water Resour. Res.* 34 (3), 409–419.
- Slattery, M.C., Bryan, R.B., 1992. Hydraulic conditions for rill incision under simulated rainfall: A laboratory experiment. *Earth Surf. Process. Landforms* 17 (2), 127–146.
- Sohrt, J., Ries, F., Sauter, M., Lange, J., 2014. Significance of preferential flow at the rock soil interface in a semi-arid karst environment. *Catena* 123, 1–10.
- Sun, L., Fang, H., Cai, Q., Yang, X., Jijun, H.E., Zhou, J.L., Wang, X., 2019. Sediment load change with erosion processes under simulated rainfall events. *J. Geograph. Sci.* 29 (6), 1001–1020.
- Trimble, S.W., Crosson, P., 2000. U.S. Soil erosion rates-myth and reality. *Science* 289 (5477), 248.
- Wang, D., Li, Z., Zeng, G., Nie, X., Liu, C., 2018. Evaluation of regionalization of soil and water conservation in China. *Sustainability* 10 (9), 3320.
- Wang, L., Liang, T., Chong, Z., Zhang, C., 2011. Effects of soil type on leaching and runoff transport of rare earth elements and phosphorous in laboratory experiments. *Environ. Sci. Pollut. Res.* 18 (1), 38–45.
- Wang, Z.G., Zhang, C., Sun, B.P., Ji, Q., Wang, C.H., 2015. Outline of soil and water conservation regionalization in China. *Soil Water Conserv. China* (12), 12–17.
- Wischmeier, W.H., 1959. A Rainfall Erosion Index for a Universal Soil-Loss Equation. *Soil Sci. Soc. Am. J.* 23 (3), 246–249.
- Wischmeier, W.H., 1976. Use and misuse of the universal soil loss equation. *J. Soil Water Conserv.* 31 (1), 5–9.
- Wischmeier, W.H., Smith, D.D., 1978. Predicting rainfall erosion losses—a guide to conservation planning. USDA, Agriculture Handbook No. 537. US. Govt. Printing Office, Washington DC, USA.
- Wolkerstorfer, G., Strauss, P., 2004. Soil erosion at the mesoscale: comparison of two erosion models for a pre-alpine Austrian basin. In: Golosov, V., Belyaev, V., Walling, D.E. (Eds.), *Sediment Transfer Through The Fluvial System*. IAHS Publ., Wallingford, UK, pp. 339–344.
- Wu, B., Wang, Z., Zhang, Q., Shen, N., Liu, J., 2017a. Modelling sheet erosion on steep slopes in the loess region of China. *J. Hydrol.* 553, 549–558.
- Wu, L., Jiang, J., Li, G.X., Ma, X.Y., 2018. Characteristics of pulsed runoff-erosion events under typical rainstorms in a small watershed on the Loess Plateau of China. *Sci. Rep.* 8 (1), 3672.
- Wu, X.L., Wei, Y.J., Wang, J.G., Xia, J.W., Cai, C.F., Wu, L.L., Fu, Z.Y., Wei, Z.Y., 2017b. Effects of erosion degree and rainfall intensity on erosion processes for Ultisols derived from quaternary red clay. *Agricul. Ecosyst. Environ.* 249, 226–236.
- Yang, J., Nie, Y., Chen, H., Wang, S., Wang, K., 2016. Hydraulic properties of karst fractures filled with soils and regolith materials: Implication for their ecohydrological properties. *Geoderma* 276, 93–101.
- Yang, Z.C., Ke, Q.H., Ma, Q.H., Cao, Z.H., Zhang, K.L., 2021. Response of Soil Moisture to Rainfall on Karst Yellow Soil Slope. *J. Soil Water Conserv.* 35 (2), 75–79.
- Zambon, N., Johannsen, L.L., Strauss, P., Dostal, T., Zumr, D., Cochran, T.A., Klik, A., 2021. Splash erosion affected by initial soil moisture and surface conditions under simulated rainfall. *Catena* 196, 104827.
- Zhang, K., Lian, L., Zhang, Z., 2016. Reliability of soil erodibility estimation in areas outside the US: a comparison of erodibility for main agricultural soils in the US and China. *Environ. Earth Sci.* 75 (3), 252.
- Zhang, K.L., Liu, B.Y., Cai, Y.M., 2000. The standard of unit plot in soil loss prediction of China. *Geograph. Res.* 19 (3), 297–302.
- Zhang, X.C., Nearing, M.A., Risso, L.M., McGregor, K.C., 1996. Evaluation of WEPP runoff and soil loss predictions using natural runoff plot data. *Trans. ASAE* 39 (3), 855–863.
- Zhao, Y.M., Gao, X.F., Jiang, H.T., 2013. Content of five main soil water-stable aggregates in China. *Soil Water Conserv. China* (4), 32–36.
- Zhong, S.Q., Han, Z., Du, J., Ci, E., Ni, J.P., Xie, D.T., Wei, C.F., 2019. Relationships between the lithology of purple rocks and the pedogenesis of purple soils in the Sichuan Basin, China. *Sci. Rep.* 9, 13272.
- Zhu, L., Fan, D., Ma, R., Zhang, Y., Zha, Y., 2018. Experimental and numerical investigations of influence on overland flow and water infiltration by fracture networks in soil. *Geofluids* 2018, 7056858.